Design Optimization of a Point Absorber and Hydraulic Power Take-Off Unit for Wave Energy Converter

Kurniawan T. Waskito[1,2**], Juan A.C. Siahaan[1], Muhamad A.N. Chuzain[1], Yanuar[1*], Sumit Pal[3]

[1]*Department of Mechanical Engineering, Universitas Indonesia, 16424, Depok, Indonesia*
[2]*Tropical Renewable Energy Center (TREC), Faculty of Engineering, Universitas Indonesia, 16424, Depok, Indonesia*
[3]*TU Delft Wind Energy Institute (DUWIND), Kluyverweg 1, 2629 HS Delft, The Netherland*

Abstract. In recent times, the point absorber Wave Energy Converter (WEC) has gained popularity due to its practicality. Investigating the parameters of the Hydraulic Power Take-Off (HPTO) in the WEC, including hose diameter and check valve variations, is crucial. This study analyzes optimization using the Sequential Quadratic Programming (SQP) method in MATLAB/SimScape, leading to a more comprehensive understanding of the interactions among HPTO components, such as hydraulic cylinders, check valves, hoses, accumulators, motors, and generators. Key system performance indicators, including pressure drop, flow rate, and power output, were assessed in both single and two-point absorber HPTO configurations. The optimization process yielded a maximum hydraulic power output of 7.33 kW, a mechanical power output of 6.41 kW, and an electrical power output of 5.4 kW using a 2-inch hose diameter. Additionally, utilizing a two-point absorber model enhanced power generation capacity by 47.4%, reaching 9.45 kW. The findings highlight the significant pressure drop at the check valve, with the 2-inch hose model experiencing a drop of 31.874 bar. These results demonstrate that optimizing HPTO parameters can significantly improve the efficiency of converting wave energy into electricity, providing valuable design recommendations for WEC technology.

Keywords: Design optimization; Hydraulic power take-off; Hose diameter; Sequential quadratic programming; Wave energy converter

1. Introduction

Many contemporary power plants predominantly rely on conventional energy sources. However, a notable drawback associated with this approach is the considerable emissions generated, which inflict detrimental effects on the environment. Consequently, there exists a progressive trend towards adopting renewable energy sources that manifest a markedly diminished ecological footprint (Drew, Plummer, and Sahinkaya, 2009). Utilizing ocean space as source of renewable energies, such as solar (Sofyan *et al.,* 2017), wind (Cho, Jeong, and Sari, 2011), and wave energies (Ariefianto, Hadiwidodo, and Rahmawati, 2022; Pecher, 2017) can have significant impacts, particularly on those living in coastal areas and remote

islands. Among the promising alternatives, the employment of sea wave energy conversion (WEC) stands out. Given that the Earth's vast oceans cover approximately 70% of its surface, the potential for energy generation through this method is truly substantial. This potential, if effectively harnessed, holds the promise of not only substituting conventional energy sources but also making a substantial contribution to global electricity supply. The Indonesian archipelago, notably the southern Java Sea region, holds considerable untapped potential for wave energy production (Rizal and Ningsih, 2022; Purwanto *et al.,* 2021; Wahyudie *et al.,* 2020; Kusuma, 2018; Prasetyo, Kurniawan, and Komariyah, 2018), while the cost analysis is also studied in the coast of Pacific (Bosserelle, Reddy, and Krüger, 2016). Despite the potential, the exploration of ocean wave energy to meet Indonesia's electricity demands has not been thoroughly investigated (Langer, Quist, and Blok, 2021). Nevertheless, with extensive research and effective utilization, this resource could become a crucial alternative energy source for Indonesia's future energy needs.

The literature review highlights the significance of a robust Power-Take Off (PTO) system in efficiently converting ocean wave energy into electrical power (Jahangir, Alimohamadi, and Montazeri, 2023; Wang, Isberg, and Tedeschi, 2018; Drew, Plummer, and Sahinkaya, 2009). It specifically emphasizes the suitability of Hydraulic Power Take-Off (HPTO) systems due to their compatibility with high power-to-frequency ratios and low-frequency ocean environments. This assertion is supported by references such as (Veerabhadrappa *et al.,* 2022; Jusoh *et al.,* 2019; Gaspar *et al.,* 2018; Hansen, Kramer, and Vidal, 2013; Marquis, Kramer, and Frigaard, 2010; Drew, Plummer, and Sahinkaya, 2009). Hydraulic systems are favored for their adaptability, and various configurations of HPTO systems are discussed, including Discrete Displacement HPTO (Penalba, Cortajarena, and Ringwood, 2017; Penalba *et al.,* 2017; Penalba and Ringwood, 2016; Hansen, Kramer, and Vidal, 2013), Multi-point Absorber (Do, Dang, and Ahn, 2018; Hansen and Pedersen, 2016; Hansen, 2013), Double Acting Cylinder (Sotoodeh, 2022; Antolín-Urbaneja *et al.,* 2015; Lin *et al.,* 2015) and multi-chamber cylinder (Li *et al.,* 2022). These systems, along with various parameter configurations (Jusoh *et al.,* 2022; 2021), underscore hydraulic systems' versatility in WEC.

Furthermore, the review emphasizes the importance of evaluating the performance of valves and hoses, pivotal components in the HPTO setup, to understand fluid flow dynamics and pressure distribution within the system. However, it does not explicitly compare the performance or effectiveness of different types of valves and hoses, which could be a potential avenue in this research.

The necessity for a more efficient and economical approach to optimize HPTO systems for maximum power generation needs to be investigated. To advance WEC with HPTO, the stability and energy absorption mechanisms of the HPTO system need refinement. The optimal design of the kinematics of the floating arm cylinder plays a pivotal role in the HPTO system. It plays a pivotal role in achieving optimal power generation. Therefore, it is essential to accurately estimate each component, as mentioned in the study by (Waskito *et al.,* 2024). However, determining parameter values for each HPTO component poses a challenge. Experimental methods for determining these parameters require distinct components with different specifications, entailing significant costs.

In this study, we employ the Sequential Quadratic Programming (SQP) numerical optimization method to estimate parameter values for each component of the Hydraulic Power Take-Off (HPTO) system, specifically focusing on the check valve and hose. Unlike traditional experimental methods, SQP offers advantages such as handling nonlinear relationships, constrained optimization, smooth and continuous functions, iterative refinement, handling multiple design variables, global convergence, and incorporation of

sensitivity analysis. By leveraging SQP, the study aims to identify parameter combinations that maximize power output and consider existing constraints effectively and economically. This systematic approach represents a novel method for optimizing HPTO systems in WECs, thereby addressing the research gap and contributing to the advancement of wave energy conversion technologies.

2. Methods

This section describes the methods for modeling the floating absorbers and HPTO. It begins by modeling the WEC with the HPTO unit, providing a mechanical overview of the WEC. Next, it describes the mathematical formulation of the HPTO and the parameter optimization process using Sequential Quadratic Programming.

2.1. Modeling the WEC with HPTO Unit: An Overview

The evaluation and presentation of the HPTO is initiated by outlining its layout and key components. This includes a description of the HPTO's main features and overall operation. The HPTO with Double Acting Cylinder (DAC) was selected based on its component efficiency and power generation capabilities. In this system, the floating absorber is connected to a fixed body to capture the kinetic energy of ocean waves effectively. The HPTO system is coupled with floating absorbers to convert mechanical energy into usable electrical power. Figure 2 displays the floating absorber system with a Hydraulic Power Take-Off unit. This unit comprises a Hydraulic Motor (HM), Check Valve (CV), High-Pressure Accumulator (HPA), Low-Pressure Accumulator (LPA), and a generator (G). In this design, the floating absorber's arm experiences reciprocating motion in response to pitch and heave motions caused by ocean waves at certain frequencies. This arm motion actuates the cylinder mechanism, generating pressure in each chamber. This pressure drives hydraulic fluid into the HPA via hydraulic hoses and check valves (CV1 and CV3). The pressurized fluid is then directed to the HM. Any excess pressure from the hydraulic motor is stored in the LPA, subsequently re-entering the flowline input of the double-acting cylinder through CV2 and CV4.
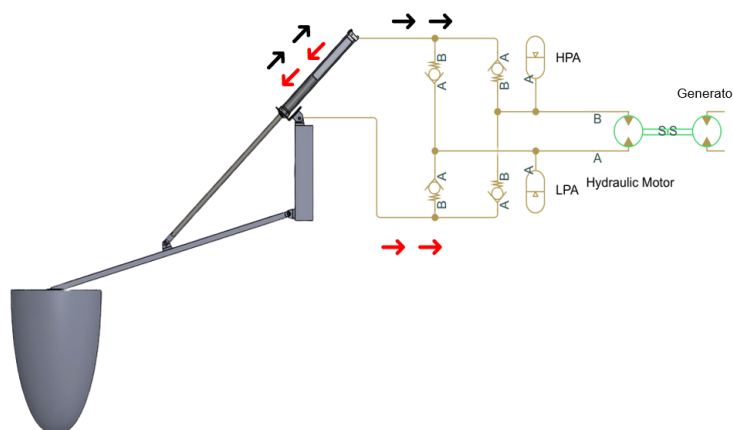

Figure 1 Design and Modeling of the WEC, Single-Point WEC System, Adapted from Waskito *et al.,* (2024)

2.2. Mechanical overview of the WEC

The geometry of the floaters can be represented as a combination of a sphere and an upper truncated cone. These floaters are primarily constructed with glass-fiber material and include a ballast chamber that can be filled through a hole located at the bottom. This chamber retains water during power generation. The ballast serves two main purposes: reducing the absorber's natural frequency and adjusting the draft of the floater as required.

Additionally, the PTO cylinders serve as a mechanism for elevating the floaters during storm protection.

The oscillating motion of the floater arm generates a moment, as depicted in Figure 3. The arm position is described by the angle θ_{arm}, which is defined to be zero when the floater is horizontal. Positive rotation is defined as the floater moving upwards. The angular velocity of the arm is denoted ω_{arm}. The PTO cylinder force is denoted Fc and the cylinder stroke xc. The length $xc, 0$ is the cylinder stroke at which the arm angle θ_{arm} is zero. The distance da is the cylinder's moment arm for applying torque to the float arm and is dependent on the angle θ_{arm}. The relation of the cylinder stroke and arm angle may be expressed in Equations (1-3),

$$xc = -cc + \sqrt{-2ac.bc \cos(\theta a - (\vartheta|_{\theta arm=0}) + ac^2 + bc^2}$$ (1)

where,

$$\vartheta|_{\theta arm=0} = cos^{-1}(\frac{ac^2 + bc^2 - (xc,0+cc)^2}{2ac.bc})$$ (2)

The cylinder's moment arm da may be expressed as:

$$da = \frac{a2.b2 \sin(\theta a - \vartheta|_{\theta arm=0})}{(xc+c2)}$$ (3)
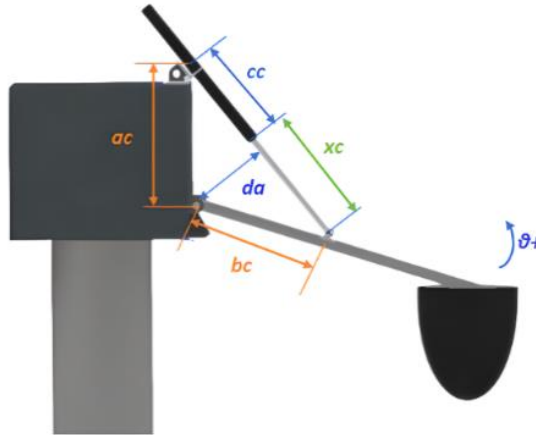

Figure 2 Floating Arm Cylinder Kinematics

The linear potential theory is used for the hydrodynamic model by solving the frequency domain. The formula is given as follows:

$$(J_{arm} + J_{add,\infty})\alpha_{arm}(t) + \int_0^t k_{rad}(t-\tau)\,\omega_{arm}(t) + k_{res}(t)\theta_{arm}(t) + M_{HPTO}(t) = \int_{-\infty}^{\infty} h_{ex}(t-\tau)\eta_W(\tau)d\tau$$ (4)

where J_{WEC} is the floater and arm moment of inertia of wave energy converter, $J_{add,\infty}$ is the added mass. α_{arm}, ω_{arm} θ_{arm}, are the angular acceleration, angular velocity, and angular position of WEC during the pitch motion. $k_{rad}(t)$ is the radiation impulse response function, τ is the time delay, k_{res} is the hydrostatic restoring coefficient, $h_{ex}(t-\tau)$ is the impulse response function, and η_W is the undisturbed wave elevation at the floater center point. The coefficients can be determined from hydrodynamic analysis using potential flow computation such as the Constant Panel Method (CPM), Higher Order Boundary Method (HOBEM), and ANSYS AQWA (ANSYS 2014; Newman 1986) (11-12). In Equation (4) the non-linear effect of HPTO is considered, so that the moment on HPTO can use Equation (5).

$$M_{HPTO} = F_{HPTO}da$$ (5)

2.3. Mathematical formulation of the HPTO model

In the HPTO unit, many parameters are considered, such as chamber piston area (A_p), piston friction (F_{fric}), the pressure of the hydraulic chamber ($p_A \& p_B$), piston acceleration ($\ddot{x}_p$), Mass of the piston, rod, and oil (M_p, M_r, M_{oil}), and gravitational acceleration (g). All equations are written in Equation (6-8).

$$F_{HPTO} = A_p(|P_A - P_B|) + F_{fric} + F_{in} \tag{6}$$

$$F_{fric} = |A_p(p_B - p_A)|(1 - F_{fric}) \tag{7}$$

$$F_{in} = \ddot{x}_p(M_p + M_r + M_{oil}) + (M_p + M_r)g \tag{8}$$

The piston chamber experiences constantly changing pressure due to the upward and downward motion. By using equations (9) and (10), it is possible to obtain dynamic values of pressure in the piston chamber by considering the effective bulk modulus (β_{eff}), in/out volumetric flow (q_A, q_B), and velocity on piston ($\dot{x}_p$). The chamber area is obtained from Equations (11) and (12). d_p and d_r are the piston and rod diameters.

$$\frac{d}{dt}p_A = \frac{\beta_{eff}}{A_{p,A}(L-x_p)}(q_A - \dot{x}_p A_{p,A}) \tag{9}$$

$$\frac{d}{dt}p_B = \frac{\beta_{eff}}{A_{p,B}(L-x_p)}(\dot{x}_p A_{p,B} - q_B) \tag{10}$$

$$A_{p,A} = \pi d_p{}^2/4 \tag{11}$$

$$A_{p,B} = \pi(d_p{}^2 - d_r{}^2)/4 \tag{12}$$

The fluid flow rectifier uses four check valves in each cylinder. In equation (13), q_{cv} is the flow through the check valve. P_{cvin} and Pcv_{out} are the pressure on the in and out section of the valve. C_d is the discharge coefficient. A_{cv} is the area of the valve. p_{oil} is the density of fluid, oil.

$$q_{CV} = \begin{cases} C_d A_{CV}\sqrt{2|p_{CVin} - p_{CVout}|, \rho_{oil}} & ,p_{CV_{in}} > p_{CV_{out}} \\ 0, else \end{cases} \tag{13}$$

High-pressure accumulators (HPA) and Low-Pressure accumulators (LPA) are essential components in maintaining pressure stability in the PTO system. Equation (14-17) is used to find the pressure and volume values of the accumulator. p_{HPA}, p_{LPA}, $p_{o,HPA}$, and $p_{o,LPA}$ are the pressure and pre-charge pressure in the HPA and LPA. $V_{HPA.}$, V_{LPA}, $V_{0,HPA,}$ and $V_{0,LPA}$ are the initial and the instantaneous volume of gas in the HPA and LPA, and γ is the adiabatic index accumulators.

$$p_{HPA}.V_{HPA}{}^{\gamma} = p_{0,HPA}.V_{0,HPA}{}^{\gamma} \tag{14}$$

$$p_{LPA}.V_{LPA}{}^{\gamma} = p_{0,LPA}.V_{0,LPA}{}^{\gamma} \tag{15}$$

$$V_{HPA}(t) = V_{0,HPA} - \int_0^t q_{HPA}\,dt \tag{16}$$

$$V_{LPA}(t) = V_{0,LPA} - \int_0^t q_{LPA}\,dt \tag{17}$$

Volumetric flow in HPA and LPA can be calculated by equations (18) and (19):

$$q_{HPA} = q_{CV_1} + q_{CV_2} - q_{HM} \tag{18}$$

$$q_{LPA} = q_{CV_3} + q_{CV_4} - q_{HM} \tag{19}$$

Equation (20) below is used to obtain volumetric flow through the hydraulic motor. $D_{HM}, \omega_{HM}, q_{HM,loss}$ are displacement, speed, and volumetric flow losses of the HM. The torque in the HM (τ_{HM}) can also be determined by Equation (21), where Δp_{HM} is the difference in pressure in HM.

$$q_{HM} = D_{HM}\omega_{HM} - q_{HM,loss} \tag{20}$$

$$\tau_{HM} = D_{HM}\Delta p_{HM} \tag{21}$$

Hoses play a crucial role in connecting different components in hydraulic systems. They facilitate the smooth flow of hydraulic fluid, which helps to convert fluid energy into mechanical energy. This process ultimately leads to the generation of electrical power. During simulations conducted in Simulink, hoses are represented as hydraulic resistive tubes, accounting for the hydraulic channel's resistance. Additionally, these hoses tend to experience pressure losses, that is subsequently simulated within Simulink using the Darcy equation as in the following Equations (22-24):

$$p = d \frac{(L+L_{eq})}{D_H} \frac{\rho}{2A^2} q.|q| \tag{22}$$

$$f = \begin{cases} \dfrac{K_s}{Re} & for\ Re \leq Re_L \\ f_L \dfrac{f_T - f_L}{Re_T - Re_L}(Re - Re_L) & for\ Re_L < Re < Re_T \\ \left(-1.8\log_{10}\left(\dfrac{6.9}{Re} + \left(\dfrac{\frac{r}{D_H}}{3.7}\right)^{1.11}\right)\right)^2 & for\ Re \geq Re_T \end{cases} \tag{23}$$

$$Re = \frac{q.D_H}{A.v} \tag{24}$$

P is Pressure loss along the pipe due to friction, q is flowrate through the pipe. Re is a Reynold Number, and Re_L, Re_T are Reynold number at laminar and turbulent flow. K_s is the shape factor that characterizes the pipe cross-section. f_L and f_T are friction factors at laminar and turbulent flow. A, D_H, and L are area, diameter, and length of pipe hydraulic. r is Height of the roughness on the pipe internal surface and, v is fluid kinematic viscosity.

2.4. Parameter Optimization of HPTO using Sequential Quadratic Programming

Figure 3 shows the flow chart of HPTO optimization process. The initial value for finding the optimal parameters in the check valve, accumulator, hose, and hydraulic motor is determined by the predetermined sizing of the hydraulic cylinders and configurations of the components.

The Hydraulic Power Take-Off (HPTO) design phase encompasses the establishment of layout, schematics, and configurations. This design process is executed using MATLAB/Simscape and Simulink software. An approach based on available manufacturer specifications is employed to determine initial component parameters, as outlined in Table 1. Simulations are conducted on the design of a single absorber to assess its performance, with simulation results compared against desired performance outputs. This iterative process involves random component selection until suitable outputs and parameters are approximatedSubsequently, these parameters are processed using the Sequential Quadratic Programming (SQP) algorithm through the Response Optimizer feature in order to optimize the HPTO design. This optimization aims to determine the most suitable parameter configurations obtained from Equation (25)

$$\nabla_x L = \nabla_x f(x) + \Sigma_i \lambda_i \nabla g_i(x) + \Sigma_j y_j \nabla h_j(x) = 0 \tag{25}$$

$\nabla_x L$ is the gradient of the Lagrangian function, $\nabla_x f(x)$ is the gradient of the objective function $f(x)$, $\Sigma_i \lambda_i \nabla g_i(x)$ is the sum of all equality constraints, $\Sigma_j y_j \nabla h_j$ is the sum of all inequality constraints. In this study, the wave model employed is that of a regular wave with a force amplitude of 20 kN and a wave frequency of 6.28 rad/s, as shown in Figure 4. This wave frequency represents a wavelength of 1.56 m, and with an absorber diameter of 0.2 m, it corresponds to λ/L = 7.8, which is around resonance frequency.
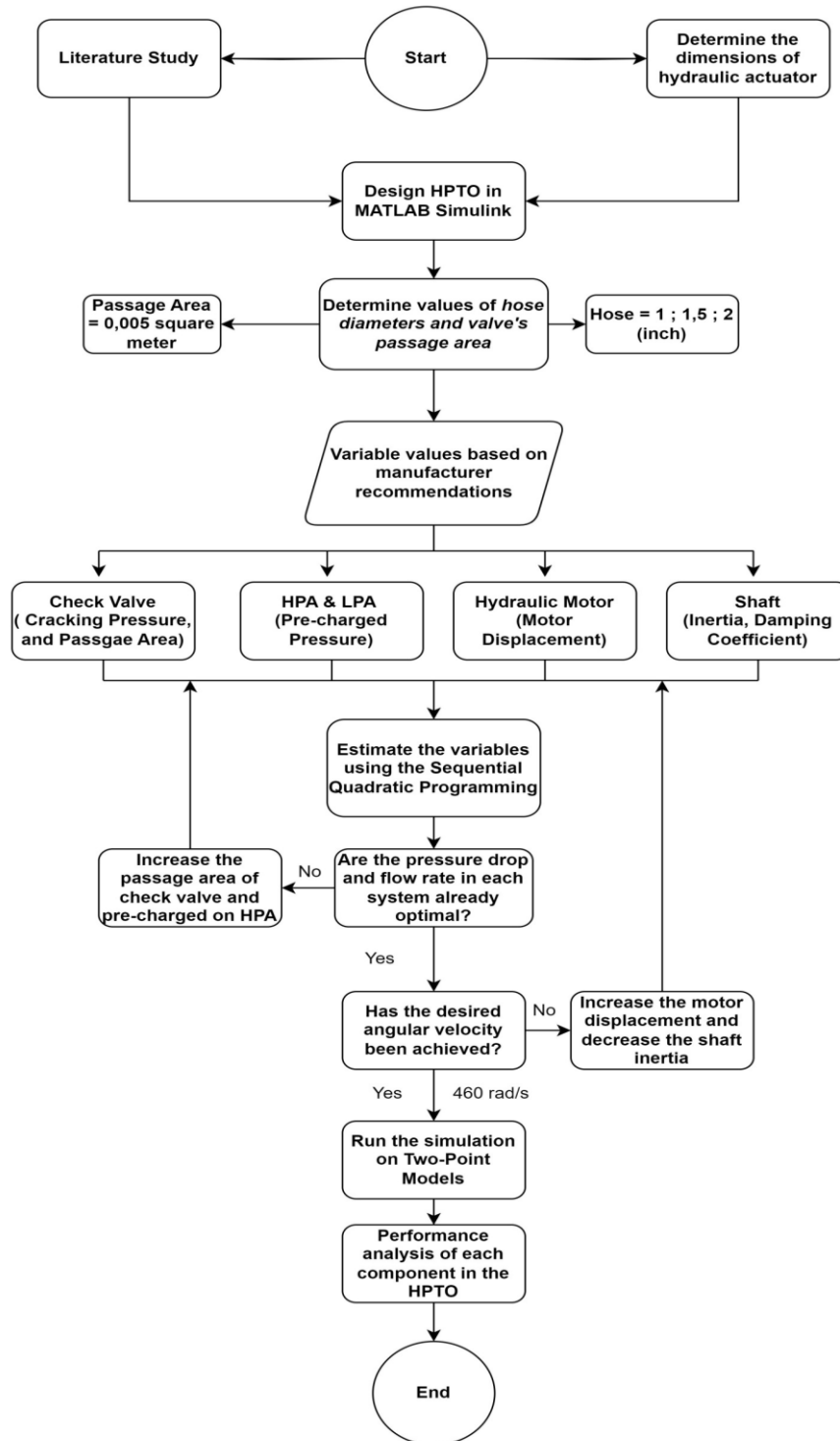

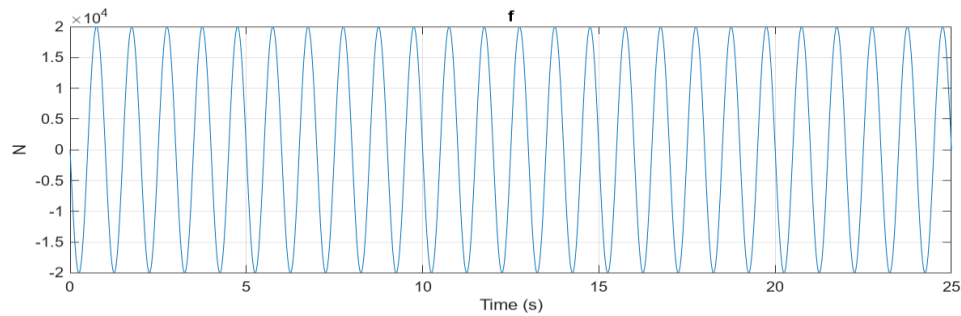**Figure 3** Flow chart of the HPTO optimization process

Figure 4 Regular sine wave force input at the hydraulic cylinder 20kN

The Response Optimizer in MATLAB software enables users to determine design parameters based on the system's response to the desired objectives. To achieve this, specific values need to be defined. This optimization aims to ensure that the motor speed does not exceed 4300 RPM or 460 rad/s. Figure 5 illustrates the angular motor speed amplitude in rad/s before optimization.
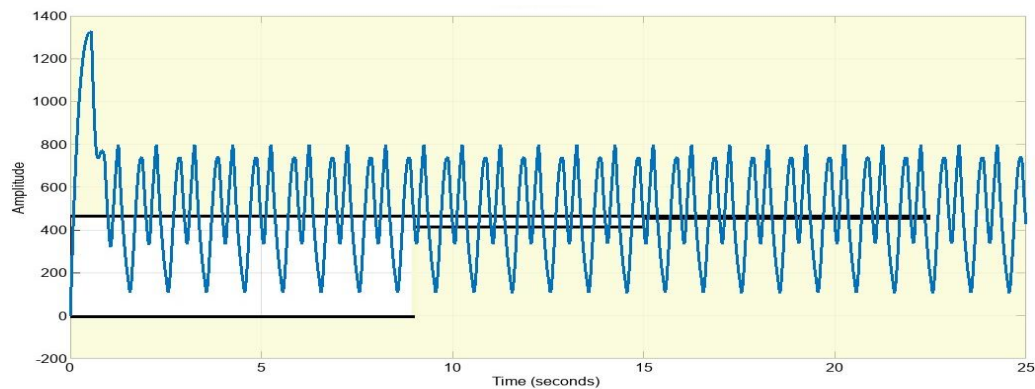

Figure 5 Angular motor speed before optimization

Table 1 comprises variables to be optimized to achieve desired values, referencing initial values provided by the manufacturer. Optimization is conducted for the design of a single-point absorber with a schematic as depicted in Figure 6. In this study, our focus lies in enhancing the generated power by analyzing the appropriate valve utilization in conjunction with hose variations of sizes 1 inch, 1.5 inches, and 2 inches. Additionally, the inlet diameter of the check valve is adjusted according to the hose size employed.

Table 1 Parameter of the HPTO model

Components	Variables	Unit	Initial Value*
Hydraulic Cylinder	Piston Area	m^2	0.0031
	Piston Stroke	m	1
Check Valve	Passage Area	m^2	0.0055
	Cracking Pressure	bar	1
	Fully Open Pressure	bar	2
Accumulator	Volume, HPA	L	50
	Volume, HPA	L	60
	Min. Volume	L	5
	Precharged Pressure, HPA	bar	50
	Precharged Pressure, LPA	bar	3
Hydraulic Motor	Displacement	cc/rev	22
	Angular Velocity	RPM	4300
Shaft	Inertia	Kg/m^2	0.01
	Damper	Kg/m^2	0.03

*Initial value obtained from the component specification provided by the manufacturer
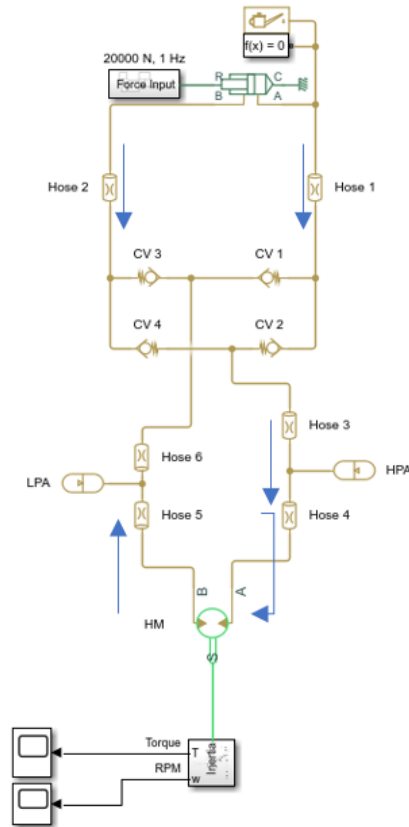
Figure 6 Schematic of the Single-Point Absorber Model in Simulink illustrates the configuration of a single-point absorber Wave Energy Converter (WEC) integrated with a Hydraulic Power Take-Off (HPTO) system

The optimization results yield recommended values for the predefined variables, with their respective values presented in Table 2. These values are obtained after the convergence of the optimization process, and they are subsequently used as input values in each Simulink block. The system is then run to assess its performance.

Table 2 Parameter of the HPTO model after optimization

| Components	Variables	Unit	Init. Value*	Aft. Opt. (1")	Aft. Opt. (1.5")	Aft. Opt. (2")
Hyd. Cylinder	Piston Area	m^2	0.0031	0.0031	0.0031	0.0031
	Piston Stroke	m	1	1	1	1
Check Valve	Passage Area	m^2	0.0055	0.0055	0.0077	0.01
	Cracking Pressure	bar	5	1.008925	1.162006	1.008783
	Max Opening Pressure	bar	2	2.0000136	1.202739	10.17489
Accumulator	Volume, HPA	L	50	45.62843	50.10132	45.59691
	Volume, HPA	L	60	45.62843	50.10132	45.59691
	Min. Volume	L	5	5	5	5
	Precharged Pressure, HPA	bar	50	39.53618	38.25947	39.25947
		bar	3	3	3	3
	Precharged Pressure, LPA					
Hyd. Motor	Displacement	cc/rev	22	25	25	25
Shaft	Inertia	Kg/m^2	0.01	0.0108	0.01	0.01
	Damper	Kg/m^2	0.03	0.033	0.031	0.033
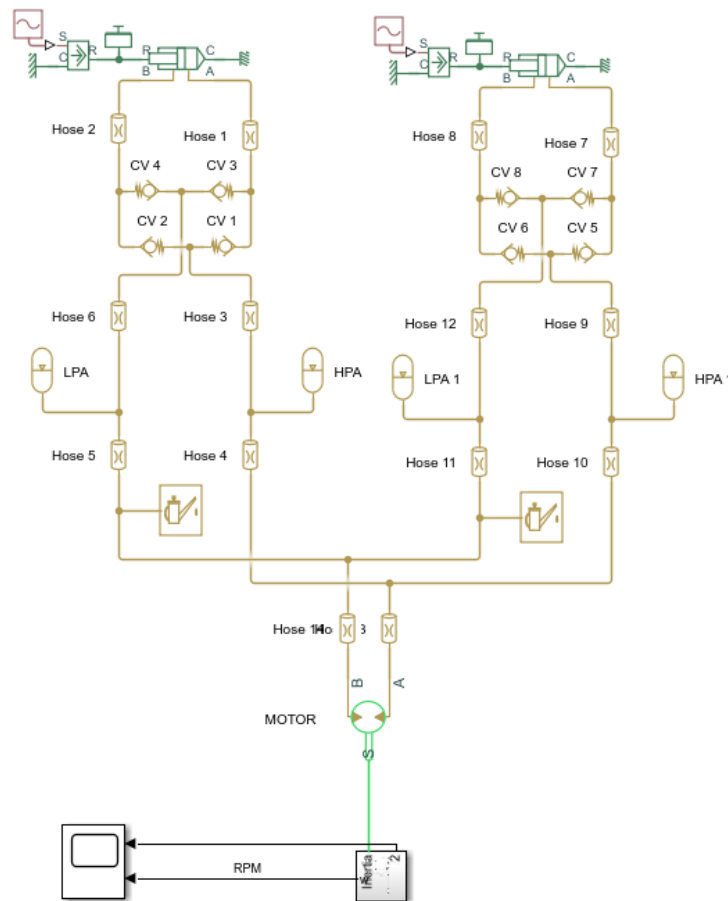
Figure 7 Schematic of the Two-Point Absorber Model in Simulink presents a two-point absorber WEC system designed for enhanced energy capture. The model highlights the dual absorber configuration and its integration with the HPTO

3.   Results and Discussion

3.1. Cylinder Kinematics of a Single Floating Absorber

The following are the results of the calculations for the arm angle, θ_{arm}, with the cylinder stroke, xc, as shown in Figure 8(a), and the moment arm, da, as shown in Figure 8(b), based on variations in the hydraulic cylinder ratio with the arm length, bc. In Figure 8(a), the arm angle is formed between 0° to 30° for a ratio of 0.84, and between -10° to 30° for a ratio of 1. This limitation in the arm angle is due to the cylinder stroke limit, which was designed to be 3.2 meters. From the graph in Figure 8(a), it is evident that as the hydraulic cylinder ratio to bc decreases, the stroke length of the cylinder increases. This indicates that a longer arm length, bc, results in a larger cylinder stroke, xc.

In Figure 8(b), a smaller hydraulic cylinder ratio with the arm length, bc, leads to a larger moment arm, da. This implies that as the ratio of the hydraulic cylinder to bc decreases, the moment the arm increases, indicating a higher mechanical advantage.
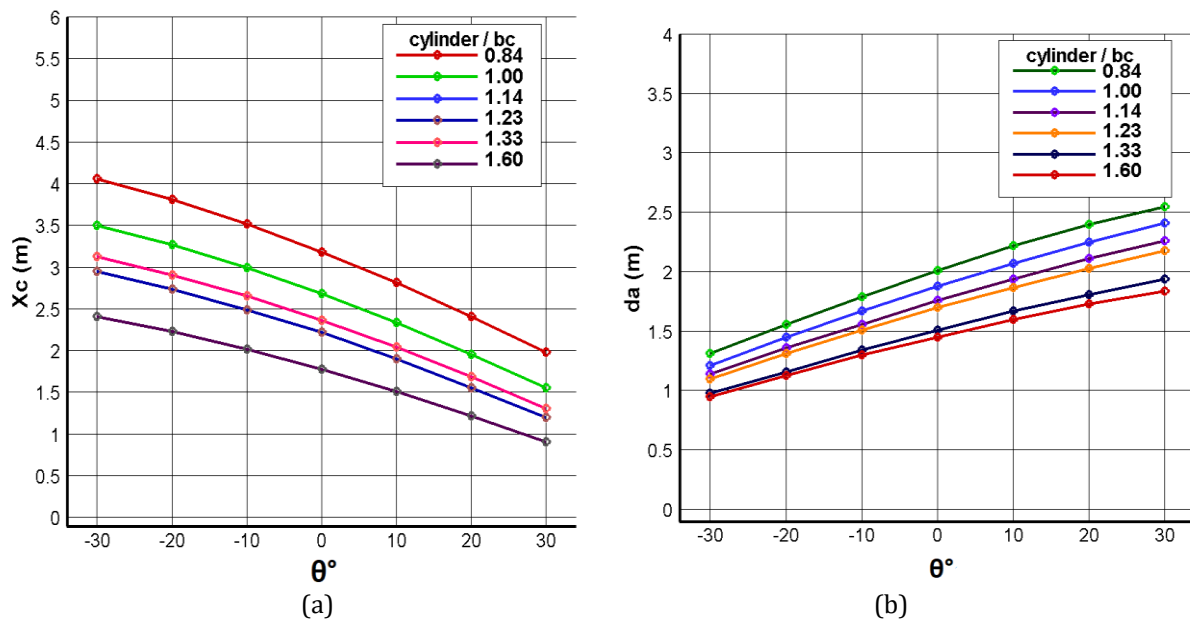
(a)

(b)

Figure 8 The Relationship Between the Arm Angle, θ, and (a) the Cylinder Stroke, xc, and (b) the Moment Arm, da.

3.2. Performance of HPTO

The double-acting cylinder initiates fluid flow from chamber A (high pressure) and chamber B (low pressure), which is directed through hoses 1 and 2, respectively. Subsequently, the high-pressure fluid encounters a barrier at CV1 before being flowed towards CV2. The flow emerging from CV2 proceeds through hose 3, the HPA, hose 4, and eventually reaches the hydraulic motor. The fluid discharged by the motor subsequently finds its way back to the cylinder by means of the LPA.

Table 3 provides a comprehensive overview of the pressure drop and volumetric flow rate across varying hose diameters. Notably, as the hose diameter increases, there is a discernible decrease in pressure drop and a corresponding increase in volumetric flow rate. Consequently, the angular velocity and torque are most pronounced for the 2-inch diameter configuration. It's worth highlighting that the primary source of substantial pressure drop occurs within the check valve, whereas the dominant flow rate manifests within the HPA.

Table 3 Summary of flow parameter data on the cylinder, hose, HPA, and motor.

Models	Pressure at cylinder (port B) (bar)	Pressure at hyd. motor (bar)	Total pressure drops (bar)	Volumetric flow rate at hose 2 (m³/s)	Volumetric flow rate at hyd. motor(m³/s)	Angular velocity (rad/s)	Torque (Nm)
1 in	69.113	36.33	32.783	0.008675	0.002175	443	13.29
1.5 in	69.15	37.06	32.09	0.009052	0.00225	456	13.68
2 in	69.124	37.06	32.064	0.009128	0.00288	460	13.7

The results presented in Figure 9 and Table 4 provide valuable insights into the performance of different configurations of Hydraulic Power Take-Off (HPTO) systems in wave energy conversion. In alignment with the details outlined in Table 3, the focus on fluid dynamic parameters, particularly angular velocity and torque, highlights their influence on hydraulic motor performance, directly impacting the overall efficiency of power generation.

Firstly, it is noteworthy that the hydraulic motor power reaches its maximum when using a 2-inch hose diameter. This indicates that the diameter of the hose plays a crucial

role in achieving optimal power output. This suggests that the diameter of the hose plays a crucial role in optimizing power output. A larger hose diameter likely allows for greater fluid flow, resulting in higher angular velocity and torque, leading to increased power generation. This finding underscores the importance of carefully selecting and optimizing the dimensions of components within the HPTO system to maximize efficiency.
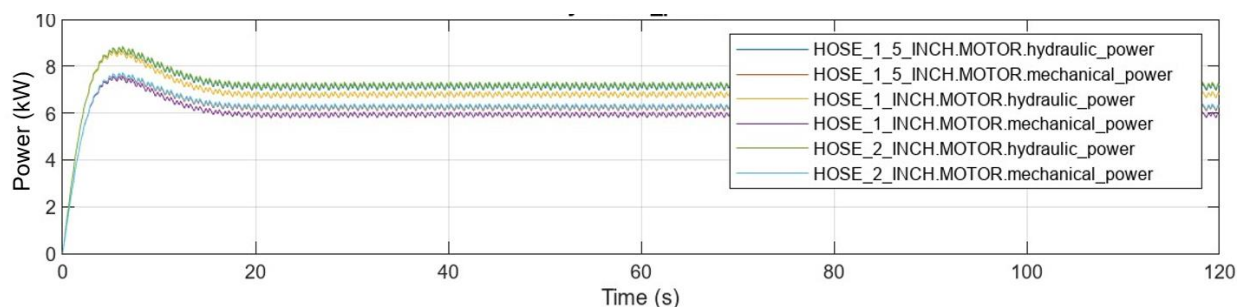

Figure 9 Torque, angular velocity, and power output at the hydraulic motor for different hose diameters

Additionally, Table 4 provides insight into the electrical power output derived from the generator for each configuration. By comparing the power output of multi-point absorbers with that of two-point absorbers, we can assess the potential for increased power generation. The inclusion of multi-point absorber configurations demonstrates the possibility of achieving higher power output through more complex absorber designs that can capture energy from multiple points along the wave's motion.

Table 4 Power output data on the motor and generator at different diameters

Models	Hydraulic power (kW)	Mechanical power (kW)	Electrical power (kW)	Mech. power of two absorbers (kW)
1 in	6,86	5,99	5.15	8,55
1,5 in	7,27	6,356	5.3	9,02
2 in	7,33	6,41	5.4	9,45

Compared to previous studies and other methods of energy conversion, this current study focuses on an in-depth analysis of fluid dynamic parameters and how they directly affect the performance of hydraulic motors. By optimizing hose diameter and absorber configurations, the study enhances power generation efficiency, thus contributing to advancements in wave energy conversion technology. The inclusion of multi-point absorber configurations further underscores the study's innovation, demonstrating the potential for increased power output through more complex absorber designs.

However, the current approach may have limitations, such as potential constraints in scalability or adaptability to diverse marine environments. Future research directions could focus on addressing these limitations by exploring alternative materials for HPTO components or optimizing designs for varying wave conditions. Additionally, investigating the integration of complementary energy conversion methodologies, such as combining wave energy conversion with tidal or wind energy, could offer further enhancements in efficiency and overall performance.

4. Conclusions

In conclusion, examining the cylinder kinematics of the WEC, a longer arm length, denoted as "*bc*," leads to an amplified cylinder stroke, "*xc*," and an extended moment arm. The optimal configuration for hose diameter and check valve passage area, yielding the highest power output, is achieved with a 2-inch hose diameter and a passage area of 0.01

m^2. This configuration yields a hydraulic power output of 7.33 kW, a mechanical power output of 6.41 kW, and an electrical power output of 5.4 kW. By employing a two-point absorber model, the power generation capacity of the 2-inch model is enhanced by 47.4%, reaching 9.45 kW. Notably, the most significant pressure drop occurs at the check valve, particularly in the 2-inch hose model, with a drop of 31.874 bar. Among the models considered, the 1-inch hose model exhibits the highest pressure drop, reaching 32.783 bar, signifying the difference between initial and final pressures entering the motor. Volumetric flow rate experiences significant fluctuations in the accumulator, as hydraulic fluid is filled and discharged prior to reaching the motor. The most substantial volumetric flow rate is achieved with the 2-inch hose model, owing to its larger hose volume, thereby resulting in a greater volumetric flow rate.

Acknowledgments

References

ANSYS, 2014. Aqwa Theory Manual Third-Party Software. Available online at http://www.ansys.com, Accessed on February 25, 2023

Antolín-Urbaneja, J.C., Cortés, A., Cabanes, I., Estensoro, P., Lasa, J., Marcos, M., 2015. Modeling Innovative Power Take-Off Based on Double-Acting Hydraulic Cylinders Array for Wave Energy Conversion. *Energies,* Volume 8(3), pp. 2230–2267

Ariefianto, R.M., Hadiwidodo, Y.S., Rahmawati, S., 2022. Experimental Study of a Wave Energy Converter Using a Unidirectional Cascaded Gear System in a Short-Wave Period. *International Journal of Technology,* Volume 13(2), pp. 321–331

Bosserelle, C., Reddy, S., Krüger, J., 2016. *Waves and Coasts in The Pacific Cost Analysis of Wave Energy in The Pacific.* Fiji: Pacific Community (SPC)

Cho, K.-P., Jeong, S.-H., Sari, D.P., 2011. Harvesting Wind Energy from Aerodynamic Design for Building Integrated Wind Turbines. *International Journal of Technology*, Volume 3, pp. 189–198

Do, H.T., Dang, T.D., Ahn, K.K., 2018. A Multi-Point-Absorber Wave-Energy Converter for The Stabilization of Output Power. Ocean Engineering, Volume 161, pp. 337–349

Drew, B., Plummer, A.R., Sahinkaya, M.N., 2009. A Review of Wave Energy Converter Technology. *In:* Proceedings of The Institution of Mechanical Engineers*, Part A: Journal of Power and Energy,* Volume 223(8), pp. 887–902

Gaspar, J.F., Calvário, M., Kamarlouei, M., Soares, C.G., 2018. Design Tradeoffs of an Oil-Hydraulic Power Take-Off for Wave Energy Converters*. Renewable Energy,* Volume 129, pp. 245–259

Hansen, A.H., Pedersen, H.C., 2016. Optimal Configuration of a Discrete Fluid Power Force System Utilised in the PTO for WECs. *Ocean Engineering,* Volume 117, pp. 88–98

Hansen, R.H., 2013. *Design and Control of the PowerTake-Off System for a Wave Energy Converter with Multiple Absorbers.* Department of Energy Technology, Aalborg University

Hansen, R.H., Kramer, M.M., Vidal, E., 2013. Discrete Displacement Hydraulic Power Take-Off System for The Wavestar Wave Energy Converter. *Energies,* Volume 6(8), pp. 4001–4044

Jahangir, M.H., Alimohamadi, R., Montazeri, M., 2023. Performance Comparison of Pelamis, Wavestar, Langley, Oscillating Water Column and Aqua Buoy Wave Energy Converters Supplying Islands Energy Demands. *Energy Reports,* Volume 9, pp. 5111–5124

Jusoh, M.A., Ibrahim, M.Z., Daud, M.Z., Albani, A., Yusop, Z.M., 2019. Hydraulic Power Take-Off Concepts for Wave Energy Conversion System: A Review. *Energies,* Volume 12(23), p. 4510

Jusoh, M.A., Ibrahim, M.Z., Daud, M.Z., Yusop, Z.M., Albani, A., 2021. An Estimation of Hydraulic Power Take-Off Unit Parameters for Wave Energy Converter Device Using Non-Evolutionary NLPQL and Evolutionary GA Approaches. *Energies,* Volume 14(1), p. 79

Jusoh, M.A., Yusop, Z.M., Albani, A., Daud, M.Z., Ibrahim, M.Z., 2022. An Improved Hydraulic Power Take-Off Unit Based on Dual Fluid Energy Storage for Reducing the Power Fluctuation Problem in the Wave Energy Conversion System. *Journal of Marine Science and Engineering,* Volume 10(8), p. 1160

Kusuma, A., 2018. *Ocean Energy Overview: Feasibility Study of Ocean Energy Ocean Energy Overview: Feasibility Study of Ocean Energy Implementation in Indonesia Implementation In Indonesia*. Dissertation, World Maritime University

Langer, J., Quist, J., Blok, K., 2021. Review of Renewable Energy Potentials in Indonesia and Their Contribution to a 100% Renewable Electricity System. *Energies,* Volume14(21), p. 7033

Li, C., Zhang, D., Zhang, W., Liu, X., Tan, M., Si, Y., Qian, P., 2022. A Constant-Pressure Hydraulic PTO System for a Wave Energy Converter Based on a Hydraulic Transformer and Multi-Chamber Cylinder. *Energies,* Volume 15(1), p. 241

Lin, Y., Bao, J., Liu, H., Li, W., Tu, L., Zhang, D., 2015. Review of Hydraulic Transmission Technologies for Wave Power Generation. Renewable and Sustainable Energy Reviews, Volume 50, pp. 194–203

Marquis, L., Kramer, M., Frigaard, P., 2010. First Power Production Figures From The Wave Star Roshage Wave Energy Converter. *In:* Proceedings of the 3rd International Conference on Ocean Energy, Volume 68, pp. 1–5

Newman, J.N., 1986. Distributions of Sources and Normal Dipoles Over a Quadrilateral Panel. *Journal of Engineering Mathematics,* Volume 20(2), pp. 113–126

Pecher, A., 2017. *Handbook of Ocean Wave Energy.* Volume 7. Springer International Publishing

Penalba, M., Cortajarena, J.A., Ringwood, J.V., 2017. Validating a Wave-To-Wire Model for a Wave Energy Converter-Part II: The Electrical System. Energies, Volume 10(7), p. 977

Penalba, M., Ringwood, J.V., 2016. A Review of Wave-To-Wire Models for Wave Energy Converters. *Energies,* Volume 9(7), p. 506

Penalba, M., Sell, N.P., Hillis, A.J., Ringwood, J.V., 2017. Validating A Wave-To-Wire Model For A Wave Energy Converter-Part I: The Hydraulic Transmission System. *Energies,* Volume 10(7), p. 977

Prasetyo, F.A., Kurniawan, M.A., Komariyah, S., 2018. Indonesian Seastate Condition and Its Wave Scatter Map. *In*: Proceeding of Marine Safety and Maritime Installation (MSMI 2018), pp. 68–79

Purwanto, P., Sugianto, D. N., Zainuri, M., Permatasari, G., Atmodjo, W., Rochaddi, B., Ismanto, A., Wetchayont, P., Wirasatriya, A., 2021. Seasonal Variability of Waves Within the Indonesian Seas and Its Relation With the Monsoon Wind. *Indonesian Journal of Marine Sciences/Ilmu Kelautan,* Volume 26(3), pp. 189–196

Rizal, A.M., Ningsih, N.S., 2022. Description and Variation of Ocean Wave Energy in Indonesian Seas and Adjacent Waters. *Ocean Engineering*, Volume 251, p.111086

Sofyan, N., Ridhova, A., Yuwono, A.H., Udhiarto, A., 2017. Fabrication of Solar Cells with TiO_2 Nanoparticles Sensitized Using Natural Dye Extracted from Mangosteen Pericarps. *International Journal of Technology,* Volume 8(7), pp. 1229–1238

Sotoodeh, K., 2022. Using Double-acting Hydraulic Actuators for Weight Reduction in the Offshore Industry. *Journal of Marine Science and Application,* Volume 21(2), pp. 159–169

Veerabhadrappa, K., Suhas, B.G., Mangrulkar, C.K., Kumar, R.S., Mudakappanavar, V.S., Seetharamu, K.N., 2022. Power Generation Using Ocean Waves: A Review. *Global Transitions Proceedings*, Volume 3(2), pp. 359–370

Wahyudie, A., Susilo, T.B., Alaryani, F., Nandar, C.S.A., Jama, M.A., Daher, A., Shareef, H., 2020. Wave Power Assessment in the Middle Part of the Southern Coast of Java Island. *Energies,* Volume 13(10), p. 2633

Wang, L., Isberg, J., Tedeschi, E., 2018. Review Of Control Strategies For Wave Energy Conversion Systems And Their Validation: The Wave-To-Wire Approach. *Renewable and Sustainable Energy Reviews*, Volume 81, pp. 366–379

Waskito, K.T., Geraldi, A., Ichi, A.C., Yanuar, Rahardjo, G.P., Al Ghifari, I., 2024. Design of Hydraulic Power Take-Off Systems Unit Parameters for Multi-Point Absorbers Wave Energy Converter. *Energy Reports,* Volume 11, pp. 115–127